DNA repair and gene targeting in plant end-joining mutants

Jia, Q.

Chapter 3

Poly(ADP-ribose) polymerase facilitating back-up non-homologous end joining via micro-homologous sequences in plants

Qi Jia, B. Sylvia de Pater and Paul J.J. Hooykaas

Abstract

Poly(ADP-ribose) polymerase 1 (Parp1) and Parp2 are ADP-ribose transferases, which are involved in single strand break repair (SSBR), base excision repair (BER) and back-up NHEJ (B-NHEJ) in animals. In order to investigate if Parp has similar functions in plants, two Arabidopsis lines with a T-DNA insertion in *AtParp1* and *AtParp2* were functionally characterized. The homozygous mutants of *Atparp1*, *Atparp2* and *Atparp1parp2* (*Atp1p2*) were phenotypically indistinguishable from the wild-type under normal growth conditions. However, the *Atparp1* and *Atp1p2* mutants were hypersensitive to the genotoxic agent MMS, but not to bleomycin, suggesting that AtParp1 has an important role in SSB DNA repair. *AtParp2* was up-regulated in NHEJ mutants, suggesting that AtParp2 may also be involved in double strand break (DSB) repair. Indeed the capacity of DNA end joining was slightly reduced in *Atparp* mutants. In the *Atp1p2* double mutant a clear shift in end-joining was seen, utilizing significantly less micro-homology mediated end joining (MMEJ) than the wild-type. This indicates that AtParp1 and AtParp2 are functionally redundant and may cooperate in MMEJ. *Agrobacterium* mediated T-DNA transformation via floral dip was hardly affected in the *Atparp* mutants, indicating that the classical NHEJ (C-NHEJ) and/or other components play the major role in that process.

Introduction

Poly(ADP-ribose) polymerases (Parps) are ADP-ribose transferases that transfer ADP-ribose (PAR) from NAD^+ to target proteins (1;2). There are eighteen known members identified in the superfamily by *in silico* homology searching in animals (3). They share a conserved catalytic domain and an active site formed by a highly conserved sequence. Parp proteins have a major impact on various cellular processes, such as cell death, transcription, cell division, DNA repair and telomere integrity, via poly(ADP-ribosyl)ation (4). Only two of them are activated in response to DNA damage: Parp1 (113 kDa) and Parp2 (62 kDa) (5). Parp1 is involved in DNA single strand break repair (SSBR) and base excision repair (BER), preventing the formation of DNA double strand breaks (DSBs) (6-8). Parp can also attract Mre11 to sites of DNA damage to repair (9;10). Some reports also suggested that when the DNA-PK dependent classical non-homologous end joining (C-NHEJ) pathway is deficient, Parp together with Lig3 plays a role in DSB repair via back-up non-homologous end joining (B-NHEJ) (11-14). This alternative NHEJ pathway preferentially utilizes micro-homology for repair, and therefore has been called micro-homology mediated end joining (MMEJ).

Homologues of Parp1 and Parp2 have been identified in plants (15). One is the classical zinc finger containing polymerase (ZAP), which was first purified from maize seedlings and has a molecular mass of 113 kDa (16). It was also identified in Arabidopsis. ZAP has high similarity in the sequence and domain organization to Parp1 in animals (15). The other one

is a structurally non-classical Parp protein, called APP in Arabidopsis and NAP in *Zea mays* (17). It is a short version of Parp with the molecular mass of 72 kDa. The counterpart of it in animals has also been identified and was termed Parp2 (18). Since APP was identified earlier than ZAP in Arabidopsis, some people termed APP as Parp1 and ZAP as Parp2. Considering the similarity to the corresponding homologues in animals and avoiding confusion, in this chapter ZAP was termed as Parp1 and APP as Parp2. Many former reports on Parp1 and Parp2 in plants provide evidence for the function of Parp in stress tolerance and in the control of programmed cell death (19-21). As mentioned above, Parp1 and Parp2 take an important role in DNA repair in animals (4;5), whereas in plants this is still largely unknown. Parp1 and Parp2 are localized in the nucleus and are activated by DNA damage, hinting that they could also be involved in DNA repair in plants (15;22;23). In order to investigate the function of Parp proteins in DNA repair, two Col-0 Arabidopsis lines containing a T-DNA insertion in *AtParp1* or *AtParp2* genes were characterized here. The homozygous mutants of *Atparp1* and *Atparp2* were isolated and crossed with each other to obtain the homozygous double mutant of *Atparp1parp2* (*Atp1p2*). The single and double mutants were analyzed for the sensitivity to DNA damaging agents and the capacity for DNA end joining. How absence of the AtParp proteins affected *Agrobacterium*-mediated T-DNA integration via floral dip was also tested.

Material and methods

Plant material

Atparp1 and *Atparp2* T-DNA insertion lines were obtained from the GABI-Kat T-DNA collection (GABI-Kat Line 692A05) or the SALK T-DNA collection (SALK_640400), respectively. Information about them is available at http://signal.salk.edu/cgi-bin/tdnaexpress (24). The homozygotes of the *Atparp1* and *Atparp2* mutants were isolated. They were crossed to get the *Atparp1parp2* (*Atp1p2*) double mutant.

Characterization of the *Atparp1* and *Atparp2* mutants

DNA was extracted from individual plants using the CTAB DNA isolation protocol (25). The T-DNA insertion sites of the mutants were mapped with a gene-specific primer (Sp167 or Sp168 for *Atparp1*, Sp219 or Sp222 for *Atparp2*) and a T-DNA specific primer (LBb1 or Sp173 for Left Border (LB), Sp200 for Right Border (RB)). PCR products were sequenced. Pairs of gene-specific primers around the insertion site were used to determine whether the plants were homozygous or heterozygous for the T-DNA insertion. The sequences of all the primers are listed in Table 1. For Southern blot analysis, DNA from the *Atparp1* mutant was digested with EcoRV or BglII, and DNA from the *Atparp2* mutant was digested with HindIII. DNA (5 µg) was ran on a 0.7% agarose gel and transferred onto positively charged Hybond-N membrane (Amersham Biosciences). The hybridization and detection procedures were done according to the DIG protocol from Roche Applied Sciences. The

DIG probe was produced using the PCR DIG Labeling Mix (Roche) with specific primers for each T-DNA (*Atparp1* (pGABI): Sp225 and Sp226; *Atparp2* (pROK2): pROK2 and Sp250).

Table 1. Sequences of primers used for characterization of T-DNA insertion lines and Q-PCR.

Name	Locus	Sequence
LBb1	T-DNA LB	5'-GCGTGGACCGCTTGCTGCAACT-3'
Sp173	T-DNA LB	5'-CCCATTTGGACGTGAATGTAGACAC-3'
Sp200	T-DNA RB	5'-GCTTGGCTGCAGGTCGAC-3'
Sp167	*AtParp1*	5'-CATTGACGGAGATACAGAGG-3'
Sp168	*AtParp1*	5'-GGTGCAATTCTCAGTCCTTG-3'
Sp219	*AtParp2*	5'-GATGGGGAAGAGTTGGTGTG-3'
Sp222	*AtParp2*	5'-GAGTGTCTATAACAAACTGGC-3'
pROK2	pROK2 probe	5'-GCGGACGTTTTTAATGTACTGGGG-3'
Sp250	pROK2 probe	5'-GGGAATGCAGTCACCTCTAT-3'
Sp225	pGABI1 probe	5'-AAATGTAGATGTCCGCAGCG-3'
Sp226	pGABI1 probe	5'-AGACGTGACGTAAGTATCCG-3'
Sp207	*AtKu80*	5'-GCGTCTTGGAGCAGGTCTCTTC-3'
Sp208	*AtKu80*	5'-GATGAAATCCCCAGCGTTCTCG-3'
q1	*AtKu70*	5'-TCTACCACTCAGTCAACCTG-3'
q2	*AtKu70*	5'-CAATAGACAAGCCATCACAG-3'
q6	*AtLig4*	5'-GACACCAACGGCACAAG-3'
q7	*AtLig4*	5'-AAGTTCAATGTATGTCAGTCCC-3'
Sp211	*AtParp1*	5'-CTCCACTCTGTATGCGTTGGG-3'
Sp212	*AtParp1*	5'-CCCTTCTATTCATCCTCATATTATCCG-3'
Sp243	*AtParp2*	5'-CTCGGCAAGATAAGCAAGTCC-3'
Sp213	*AtXRCC1*	5'-CTTCACTACACGAGGGACAAAGC-3'
Sp214	*AtXRCC1*	5'-CAGAAACAAGGGGAACACCATCTACC-3'
Roc5.2	*Roc1*	5'-GAACGGAACAGGCGGTGAGTC-3'
Roc3.3	*Roc1*	5'-CCACAGGCTTCGTCGGCTTTC-3'
q8	BamHI	5'-GTGACATCTCCACTGACGTAAG-3'
q9	BamHI	5'-GATGAACTTCAGGGTCAGCTTG-3'
q10	GFP	5'-CAAGCTGACCCTGAAGTTCATC-3'
q11	GFP	5'-GTTGTGGCGGATCTTGAAG-3'
q30	pUC18P1/4	5'-GTTTCGGTGATGACGGTG-3'
q31	pUC18P1/4	5'-TGGCACGACAGGTTTCC-3'
q40	pUC18P1/4	5'-GCTGTAGGATGGTAGCTTGGCAC-3'
q41	pUC18P1/4	5'-ATCCTACAGCTGGAATTCGTAATC-3'

Quantitative reverse-transcription PCR (Q-RT-PCR)

Leaves of 2-week-old wild-type (ecotype Columbia-0), *Atparp1*, *Atparp2*, *Atku80*, *Atku70* and *Atlig4* plants (chapter 2) were ground under liquid N_2 in a Tissue-Lyser (Retch). Total RNA was extracted from the leaf powder using the RNeasy kit (Qiagen) according to the supplied protocol. Residual DNA was removed from the RNA samples with DNaseI (Ambion) in the presence of RNase inhibitor (Promega). RNA was quantified and 1 µg of RNA was used to make cDNA templates using the iScript cDNA synthesis kit according to the manufacturer's instructions (Bio-Rad). Quantitative real-time PCR (Q-PCR) analyses were done using the iQ™ SYBR® Green Supermix (Bio-Rad). Specific fragments (about 200 bp) were amplified with pairs of primers around the T-DNA insertion sites using a DNA Engine Thermal Cycler (MJ Research) equipped with a Chromo4 real-time PCR detection system (Bio-Rad). The sequences of the primers are listed in Table 1. The cycling parameters were 95°C for 3 min, 40 cycles of (95°C for 1 min, 60°C for 40 s), 72°C for 10 min. All sample values were normalized to the values of the house keeping gene *Roc1* (primers Roc5.2, Roc3.3) and were presented as relative expression ratios. The value of the Col-0 wild-type was set on 1.

Assays for sensitivity to bleomycin and methyl methane sulfonate (MMS)

Seeds of wild-type, *Atparp1*, *Atparp2,* and *Atp1p2* plants were surface-sterilized as described (26) and germinated on solid ½ MS medium. Four days after germination, the seedlings were transferred to liquid ½ MS medium without additions or ½ MS medium containing 0.2 µg/ml and 0.4 µg/ml Bleocin™ (Calbiochem), 0.007% and 0.01% (v/v) MMS (Sigma) and scored after 2 weeks. Fresh weight (compared with controls) was determined by weighing the seedlings in batches of 20 in triplicate, which were treated in 0%, 0.006%, 0.008% and 0.01% (v/v) MMS for 2 weeks.

Comet assay

1-week-old seedlings were treated in liquid ½ MS containing 0.01% MMS for 0 h, 2 h and 24 h. Some seedlings with 24 h treatment were recovered in liquid ½ MS for another 24 h. DNA damage was detected by comet assays as described previously (27) with minor modifications. Since MMS mostly causes SSBs, DNA was exposed to high alkali prior to electrophoresis under neutral conditions (A/N protocol) to detect DNA SSBs preferentially. Plant nuclei were embedded in 1% low melting point Ultrapure™ agarose-1000 (Invitrogen) to make a mini gel on microscopic slides according to the protocol. Nuclei were subjected to lysis in high alkali (0.3 M NaOH, 5 mM EDTA pH13.5) for 20 min at room temperature (A/N protocol). Equilibration for 3 times 5 min in TBE buffer (90 mM Tris-borate, 2 mM EDTA, pH8.4) on ice was followed by electrophoresis at 4°C (cold room) in TBE buffer for 15 min at 30 V (1 V/cm), 15-17 mA. Dry agarose gels were stained with 15 µl ethidium bromide (5 µg/ml) and immediately evaluated with a Zeiss Axioplan 2 imaging fluorescence microscope (Zeiss, Germany) using the DsRed channel (excitation at 510

nm, emission at 595 nm). Images of comets were captured at a 40-fold magnification by an AxioCam MRc5 digital camera (Zeiss, Germany). The comet analysis was carried out by comet scoring software CometScore™ (Tritek Corporation). The fraction of DNA in comet tails (%tail-DNA) was used as a measure of DNA damage. Measures included 4 independent gel replicas totaling about 100 comets analyzed per experimental point. The results were presented by the mean value (±standard deviation = S.D.) from four gels, based on the median values of %tail-DNA of 25 individual comets per gel. The student's t-test was used to test for significant difference compared to the wild-type with the same treatment.

Histochemical GUS analysis

The NHEJ mutants previously described (chapter 2) (*Atku80*, *Atku70* and *Atlig4*) were crossed with *AtParp2:GUS* reporter plants (15;28), which were kindly provided by De Veylder (Gent, Belgium). Ten-day-old seedlings were treated with 0 or 0.01% MMS for 2 h, followed by GUS staining as described previously (29). The GUS staining was examined under a Leica MZ12 microscope (Leica microsystems). Plants were photographed with a Leica DC 500 digital camera (Leica microsystems).

Isolation of Arabidopsis mesophyll protoplasts

Arabidopsis was either grown in a greenhouse at 21°C (16 h photoperiod) or in a culture chamber (21°C, 50% relative humidity, 16 h photoperiod). Rosette leaves (~1 g) from plants that were 3 to 5 weeks old were collected, rinsed with deionized water and briefly dried. The leaves were cut into 0.5 to 1 mm strips with a razor blade, placed into a Petri dish containing 15 ml of filter-sterilized enzyme solution [1.5%(w/v) cellulose R10, 0.4%(w/v) macerozyme R10, 0.4 M mannitol, 20 mM KCl, 20 mM MES pH5.7, 10 mM $CaCl_2$, 0.1%(w/v) BSA] and 2 to 3 h incubated in the dark at 28°C. Then the protoplasts were filtered with a 50 µm mesh to remove the undigested material and transferred to a round bottom Falcon tube. The solution was centrifuged for 5 min at 600 rpm to pellet the protoplasts. The supernatant which contained broken cells was discarded. The protoplasts were gently washed twice with 15 ml cold W5 solution (154 mM NaCl, 125 mM $CaCl_2$, 5 mM KCl, 2 mM MES pH5.7) and resuspended in cold W5 solution to a final concentration of 2×10^5 cells/ml and kept on ice for 30 min. Just before starting transfection, protoplasts were collected from the W5 solution by centrifugation and were resuspended to a density of 2×10^5 cells/ml in MMg solution (0.4 M mannitol, 15 mM $MgCl_2$, 4 mM MES pH5.7) at room-temperature.

End joining assay

Plasmid pART7-HA-GFP (S65T) was linearized by cleavage with BamHI (Figure1). Fresh protoplasts prepared from leaves were transformed with either linear or circular plasmid DNA by the polyethylene glycol (PEG) transformation protocol (30). In each experiment, 2×10^4 protoplasts were transformed with 2 µg of plasmid. Recircularization of the linear plasmid in

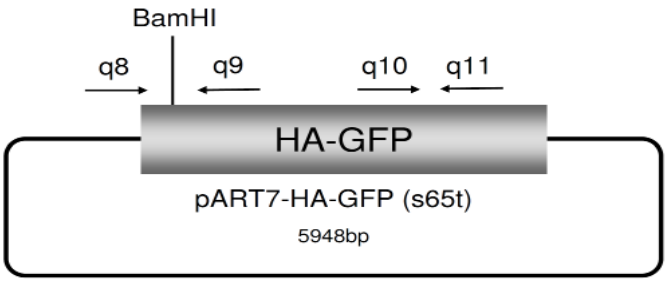

Figure 1. Schematic diagram of pART7-HA-GFP.
The primers for Q-PCR are shown by arrows.

protoplasts by the NHEJ pathway was analyzed. DNA was extracted from protoplasts (at 0 h and 20 h) and was used to quantify rejoining by Q-PCR. The DNA extraction protocol and the cycling parameters of Q-PCR were the same as mentioned above. Two pairs of primers were used: one pair (q8+q9) was flanking both sites of the enzyme digestion site (BamHI); the other pair (q10+q11) was localized in GFP (Figure1). When the plasmid is circular, both pairs will give products. When the plasmid is cleaved by BamHI, the first pair of primers will not give a product, whereas the second will still give products. The efficiency of end joining is presented by the ratio of PCR products using q8+q9 primers and q10+q11 primers in comparison with the controls. The value of Col-0 wild-type was set on 1. Q-PCR was performed as three replicates and the assays were performed in triplicate. The PCR products with the primers of q8 and q9 were purified with QIAquick gel extraction kit (Qiagen), followed by cloning into pJET1.2/blunt Cloning Vector (CloneJET^{tm} PCR Cloning Kit, Fermentas). Individual clones were first digested by BamHI. The clones resistant to the digestion of BamHI were sequenced by ServiceXS.

MMEJ assay with active protein extract from leaves

Ten-day-old seedlings were ground under liquid N_2 in a Tissue-Lyser (Retch). One ml protein extraction buffer (50 mM Tris-HCl pH 7.5; 2 mM EDTA; 0.2 mM PMSF; 1 mM DTT; 1×Protease inhibitor cocktail Complete®, EDTA free) was added to 1 g of tissue powder. Soluble protein was isolated by centrifugation at 4°C. The protein concentration was determined using Bio-Rad protein assay reagent.

The DNA substrate (pUC18P1/4) for MMEJ was described and obtained from Liang et al (31;32). The construct can be cleaved with the restriction enzymes Eco47III and EcoRV to a 2.7 kb linear form with a 10 bp direct repeat (ATCCTACAGC) at both blunt ends (Figure2). Since it was hard to digest completely, the long linear DNA fragment was amplified by PCR with q40 and q41 primers.

According to the results from Liang et al. (31;32), high DNA/protein ratio was used for the high efficiency of end joining. The linear DNA substrates (300 ng) were incubated with 1 µg protein extract from leaves in 50 mM Tris-HCl (pH 7.6), 10mM $MgCl_2$, 1mM dithiothreitol, 1 mM ATP and 25% (w/v) polyethylene glycol 2000 at 14 °C for 2 hour in a

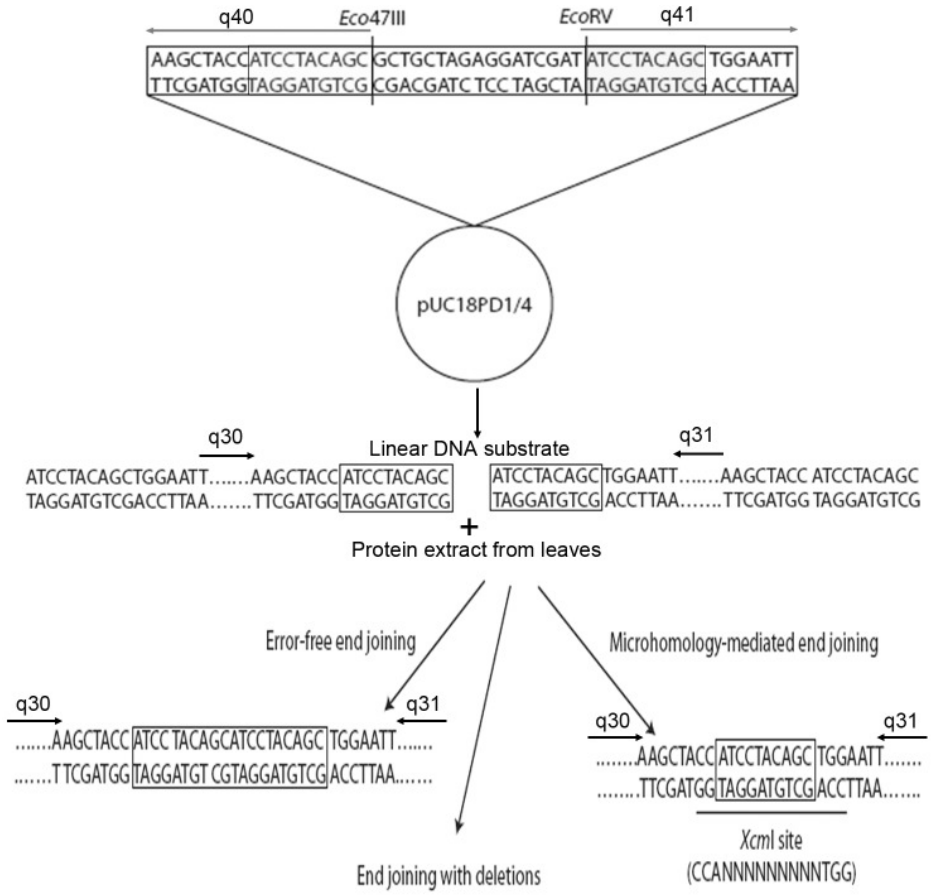

Figure2. DNA substrates for MMEJ.
The plasmid PUC18PD1/4 has two 10 bp repeats around the digestion sites of Eco47III and EcoRV. The 2.7kb linear fragment was PCR amplified with the primers (q40+q41). An XcmI restriction site will be generated after end joining via MMEJ. The primers are indicated by arrows.

volume of 20 µl. DNA products were deproteinized and purified by electrophoresis through 0.6% agarose gels. A 600-bp fragment containing the end-joined junction was amplified by PCR with q30 and q31 primers flanking the junction. When end-joining had occurred via MMEJ using the 10 bp microhomology, an XcmI site (CCAN9TGG) was generated. PCR products were digested by XcmI, followed by electrophoresis on a 1.5% agarose gel. The presence of an XcmI site will result in a 400 bp and a 200 bp fragment. The intensity of DNA bands was quantified by using ImageJ software. The relative contribution of end-joining via the 10 bp repeat was calculated as the percentage of the XcmI-digested fragments of total PCR products (sum of the XcmI- digested and undigested fragments).

Floral dip transformation

Floral dip transformation was performed according to the procedure described by Clough and Bent (33). The *Agrobacterium* strain AGL1 (pSDM3834) (34) was used for infection.

Plasmid pSDM3834 is a pCambia 1200 derivative (hpt selection marker). Seeds were harvested from the dry plants after maturation, surface-sterilized and plated on solid MA without sucrose containing 15 µg/ml hygromycin, 100 µg/ml timentin (to kill *Agrobacterium* cells) and 100 µg/ml nystatin (to prevent growth of fungi). Hygromycin-resistant seedlings were scored 2 weeks after germination and transformation frequency was determined (50 seeds is 1mg) (35).

Results

Isolation and characterization of the *Atparp1* and *Atparp2* mutants

Arabidopsis mutants with mutations in *Atparp1* and *Atparp2* were obtained from the GABI-Kat or Salk collection, respectively. We identified homozygous mutants by PCR harboring a T-DNA insertion for each gene in the next generation. When two gene-specific primers flanking the insertion site were used, PCR products were amplified for wild-type and heterozygotes. No PCR products were obtained for homozygous mutants by using these two gene-specific primers, because the PCR products in the mutant would be >10 kb in size and would be not detectable. When a T-DNA-specific primer from LB or RB was used in combination with one gene-specific primer, PCR products for the T-DNA insertion mutants were amplified, whereas no PCR products were obtained for the wild-type. The insertion point was mapped by sequencing of the PCR products generated using one of T-DNA specific primers in combination with one of the gene-specific primers. The combination of the primers for each gene is shown in the Figure 3. There were PCR products of LB and RB fragments for the *Atparp1* mutant and PCR products of two LB fragments for the *Atparp2* mutant, indicating that one T-DNA was inserted in the *AtParp1* locus and at least 2 T-DNA copies were inserted as an inverted repeat in the *AtParp2* locus. Sequencing results indicated that the T-DNAs were all inserted at the position as described in the internet database. A detailed characterization of the T-DNA insertions is shown in Figure 3. The T-DNA of *Atparp1* was integrated in exon 14 and had 240 base pairs (bps) filler DNA. The *Atparp2* line contained at least 2 T-DNA copies inserted as an inverted repeat. The T-DNA of *Atparp2* was integrated into intron 6, having 5 bps filler DNA.

The genomic DNA was digested by restriction enzymes (EcoRV or BglII for *Atparp1*, HindIII for *Atparp2*) for Southern blotting (Figure 3). If there is one T-DNA inserted in the correct locus, it can be expected that bands with the following sizes will be detected on the blot: *Atparp1*: 1350bp (EcoRV), 2716bp (BglII); *Atparp2*: 3600bp and 5476bp (HindIII). If T-DNAs are inserted in other loci, additional bands probably with different sizes will be detected. The results showed that the *Atparp1* line contained one T-DNA insertion. The expected 3600bp band for the *Atparp2* line was clearly visible, but the expected band of 5476bp for the *Atparp2* mutant was very faint, suggesting that this T-DNA was probably not intact or the digestion site of HindIII was mutated and could not be cleaved. There were four additional bands for the *Atparp2* line, indicating that this line had multiple T-DNA

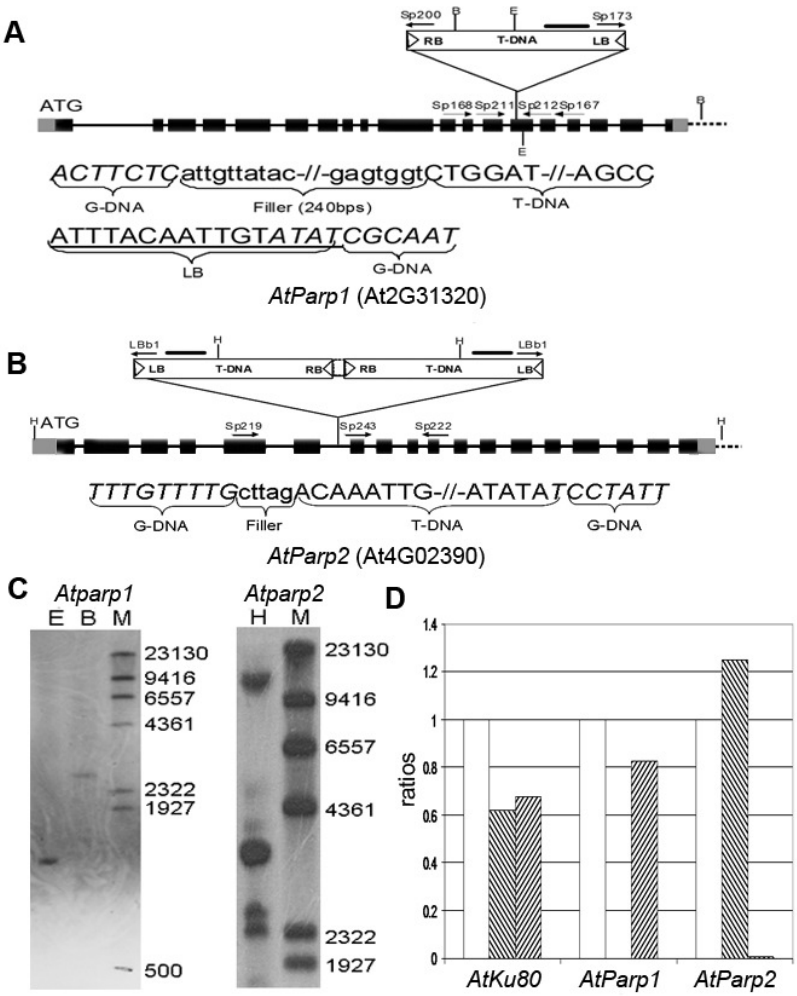

Figure 3. Molecular analysis of the T-DNA insertion in the *AtParp1* and *AtParp2* loci.
Genomic organization of the *AtParp1* (A) and *AtParp2* (B) locus are indicated with the positions of the inserted T-DNAs. Exons are shown as black boxes. 3' and 5' UTRs are shown as gray boxes. Introns are shown as lines. The primers used for genotyping and Q-RT-PCR analysis, the probes (▬) and the restriction enzyme digestion sites used for Southern blot analysis are indicated. Genomic DNA sequences (g-DNA) flanking the T-DNA insertion are shown in italic. (C) Southern blot analysis of the T-DNA insertion. The genomic DNA of the *Atparp1* mutant was digested by EcoRV (E) or BglII (B) and the DNA of the *Atparp2* mutant by HindIII (H). M: λHindIII Marker. (D) RNA expression of the *AtKu80*, *AtParp1* and *AtParp2* genes were determined by Q-RT-PCR in wild-type, *Atparp1* and *Atparp2* plants. All the sample values were normalized to *Roc* values. The values of the wild-type were set on 1.
(☐ wild-type (WT); ▨ *Atparp1*; ▨ *Atparp2*)

copies in *AtParp2* and/or extra copies located somewhere else in the genome. One band probably represents the band derived from the T-DNA copy in *Atparp2* for which no band of correct size was detected.

In order to find out whether the mutated loci still produce mRNA, Q-RT-PCR analysis was performed for the *Atparp1* and *Atparp2* T-DNA insertion lines using primers flanking the insertion site. This resulted in a product for each gene in the wild-type, but not in the corresponding T-DNA insertion mutant (Figure 3). The mRNA expression of *ku80* was also checked here as a reference. This indicated that neither of the two T-DNA insertion mutants produces a stable mRNA of the mutated gene and that the plants are homozygous mutants indeed. The *Atparp1* mutant was crossed with the *Atparp2* mutant in order to obtain double mutants. In the second generation of this cross indeed, homozygous *Atp1p2* double mutants were obtained. No obvious differences in growth were observed between the *Atparp* single or double mutants and the wild-type.

Sensitivity to bleomycin and MMS

Since more and more biochemical evidence in mammals showed that Parp1 and Parp2 are involved in DNA repair processes, we investigated whether the two Parp proteins also have a similar function in plants. To this end, the *Atparp* mutants were tested for the sensitivity to two genotoxic agents (bleomycin and MMS). The radiomimetic chemical bleomycin induces mainly DNA double strand breaks (DSBs) (36). The monofunctional alkylating agent MMS induces mainly base methylation and as a consequence DNA single strand breaks (SSBs) that can be converted into DSBs during replication (37). As shown in Figure 4, the *Atparp1* and *Atp1p2* mutants tolerated the damage induced by bleomycin equally well as the wild-type, but turned out to be hypersensitive to MMS. The *Atparp2* mutant seemed to tolerate the damage induced by both MMS and bleomycin equally well as the wild-type. This indicated that AtParp1 had an important role in SSBs repair. To quantify the effect of MMS treatment on growth, the fresh weight of seedlings was determined after 2 weeks of continuous MMS treatment. After growth on the highest concentration of MMS (0.01%) all the plant lines had become very sick and stopped growing. Lower concentrations (0.006% and 0.008%) of MMS led to growth retardation of the *Atparp1* and *Atp1p2* mutants. After growth in the presence of 0.008% MMS, the fresh weight of the *Atparp1* mutant was reduced to 2/3 of the weight of the wild-type and the fresh weight of the *Atp1p2* mutant was about 1/2 of that of the wild-type. The *Atparp2* mutant had more or less the same weight as the wild-type in all the MMS treatments. It seems that the role of AtParp2 only becomes apparent in the absence of AtParp1. When *AtParp1* is mutated as well, the effect of a mutation in *AtParp2* can be observed, since the fresh weight of the *Atp1p2* double mutant was less than that of the *Atparp1* single mutant after MMS treatment. This is in accordance with previous reports about the collaboration of Parp1 and Parp2 in efficient base excision DNA repair in mammals (38).

In order to quantify the DNA damage in these mutants after MMS treatment, comet assays (A/N protocol) were performed, measuring SSBs and DSBs. For each treatment, around 100 nuclei from 4 independent mini gel replicas were analyzed at random by using CometScore^{Tm}. Without any treatment, the *Atparp1* and *Atp1p2* mutants had already more

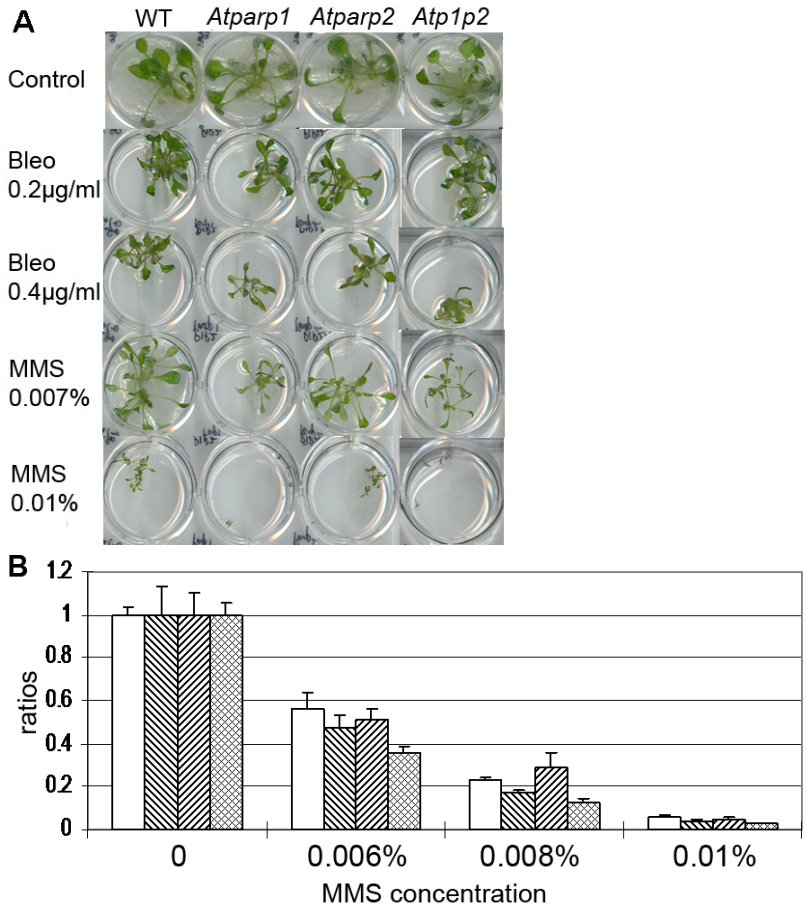

Figure 4. Response of *Atparp* mutants to DNA-damaging treatments.
(A) Phenotypes of wild-type (Col-0) plants and *Atparp1*, *Atparp2* and *Atp1p2* mutants to bleomycin or MMS treatment. Four-day-old seedlings were transferred to liquid ½ MS medium (control) or ½ MS medium containing different concentrations of bleomycin (Bleo) or MMS and were scored 2 weeks after germination.
(B) Fresh weight of 2-week-old wild-type plants and *Atparp1*, *Atparp2* and *Atp1p2* mutants treated with 0, 0.006%, 0.008% or 0.010% MMS. For each treatment 20 seedlings were weighed in triplicate. Fresh weight of the wild-type and the mutants grown for 2 weeks without MMS was set at 1. (WT; *Atparp1*; *Atparp2*; *Atp1p2*)

DNA damage than the wild-type, demonstrating that AtParp1 is involved in DNA repair (Figure 5). After 2h MMS treatment, all the mutants have more DNA damage compared to the wild-type, indicating that AtParp1 and AtParp2 are both involved in DNA repair. But the *Atparp1* and *Atp1p2* mutants had a higher level of nuclear DNA damage than the *Atparp2* mutant, suggesting that AtParp1 may have a more crucial function in SSBs repair. In both the wild-type and the mutants, the level of DNA damage after 24h MMS treatment plus 24h recovery was reduced indicative of DNA repair. Recovery was slower in the mutants than in the wild-type, and the *p1p2* mutant had slower recovery than the single *Atparp1* and

Atparp2 mutants. It seems that AtParp1 and AtParp2 have redundant functions, and that in the *Atp1p2* double mutant this function is abolished.

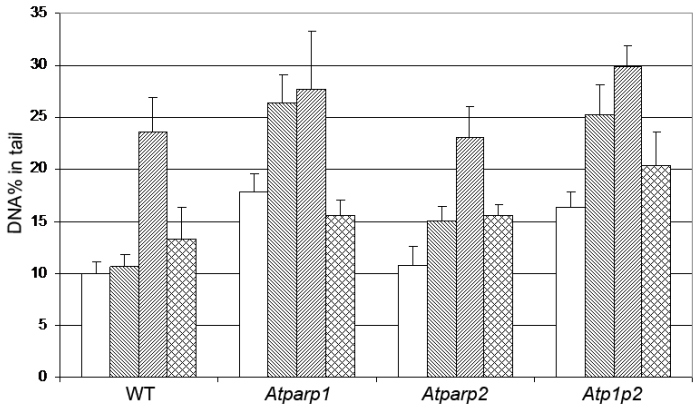

Figure 5. Comet assay.
The fraction of DNA in comet tails (%tail-DNA) was used as a measure of DNA damage in wild-type, *Atparp1*, *Atparp2* and *Atp1p2* plants. Around 100 nuclei for each treatment were analyzed at random. The means of %tail-DNA after MMS treatment are shown.
(t=0; t=2h; t=24h; 24h recovery)

The expression of *AtParp2*

Microarray analysis showed that the transcript level of *AtParp2* is induced in *Atku80* mutants and the bleomycin treated wild-type plants (23). This suggests that AtParp2 may be involved in a DNA DSB repair pathway, possibly the B-NHEJ pathway. To confirm this hypothesis, RNA expression levels of *AtParp2* and some other genes involved in DSB repair was analyzed using Q-RT-PCR in the C-NHEJ mutants (*Atku70*, *Atku80* and *Atlig4*). The results showed that the mRNA expression levels of DNA repair genes are increased in NHEJ mutants. *AtParp2* expression is increased in all mutants, and especially in the *Atlig4* mutant (Figure 6). This demonstrated that AtParp2 could be an indicator for DNA damage.

We also analyzed the expression in a *AtParp2:GUS* reporter line, which carried as transgene the *AtParp2* gene promoter fused to GUS (15;28). We crossed the *Atlig4* mutant with the *AtParp2:GUS* reporter line. The homozygous *Atlig4* mutant containing the *AtParp2:GUS* construct was obtained. MMS could induce the expression of *AtParp2* throughout the plant,

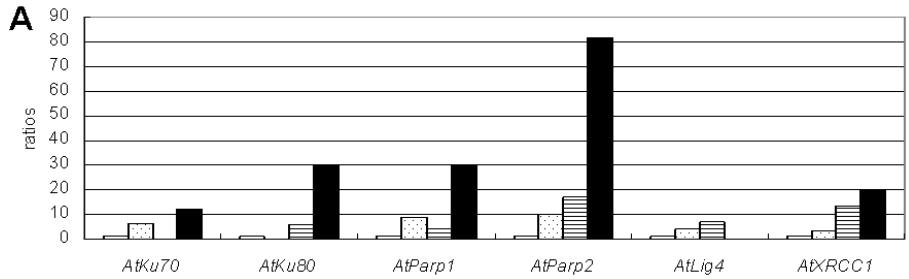

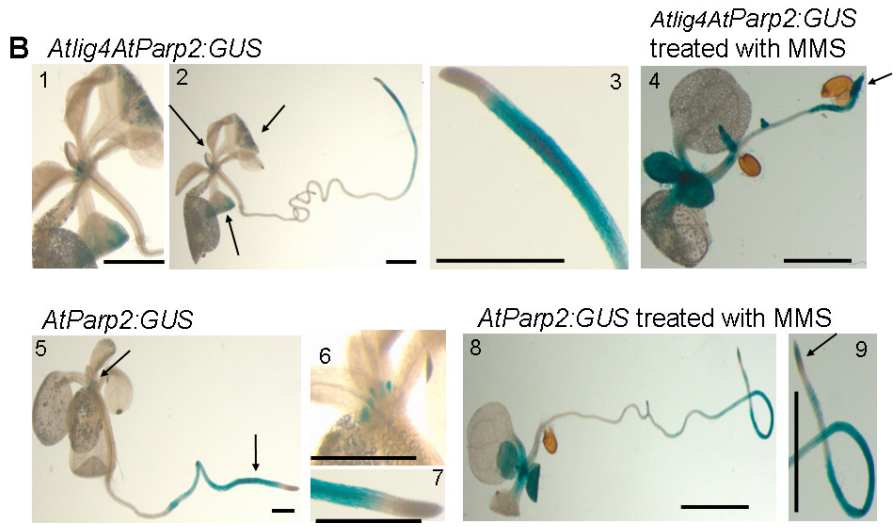

Figure 6. Parp2 expression in NHEJ mutants.
(A) RNA expression of the NHEJ genes (*AtKu70*, *AtKu80*, *AtParp1*, *AtParp2*, *AtLig4* and *AtXRCC1*) determined by Q-RT-PCR in wild-type and NHEJ mutant plants. All the values were normalized to Roc values and the ratios were obtained in triplicate. The values of the wild-type were set on 1. (□WT; ⬚*Atku80*; ▤ *Atku70*; ■*Atlig4*)
(B) Histochemical staining for GUS activity in *lig4* and wild-type seedlings harboring the *AtParp2* promoter fused to the *GUS* gene (*AtParp2:GUS*). Ten-day-old seedlings were stained for GUS expression without treatment (panel 1-3: *Atlig4AtParp2:GUS*, panel 5-7: *AtParp2:GUS*) or treated with 0.01% MMS for 2h prior to staining (panel 4: *Atlig4AtParp2:GUS*, panel 8,9: *AtParp2:GUS*). The arrows indicated the GUS expression. Bars are 3 mm.

especially in the root tip (Figure 6). The GUS staining was not significantly higher in the *Atlig4* mutant than in the wild-type (Figure 6). It may be that the *AtParp2* coding region or the sequences not present in the *AtParp2:GUS* construct are important for increased expression levels in the C-NHEJ mutants.

End joining activity

To directly test the function of *AtParp1* and *AtParp2* in NHEJ, an *in vivo* plasmid rejoining assay was utilized to quantify the capacity of the *Atparp1* and *Atparp2* mutants to repair DSBs generated by restriction enzymes. To this end, we transformed protoplasts from leaves with circular (control) or BamHI linearized plasmid DNA. BamHI digests the plasmid DNA in the N-terminal part of the GFP coding sequence. Rejoining of linear plasmid by the NHEJ pathway *in vivo* will result in GFP expression. GFP fluorescence was indeed detected in the wild-type protoplasts which were transformed with the linearized plasmid. But it was difficult to quantify the difference in GFP expression between the wild-type and the mutants under the fluorescence microscope. Therefore, we analyzed the rejoining efficiency by Q-PCR, using primers around the BamHI site and compared with primers in the GFP coding region. The results showed that the rejoining efficiencies were reduced mildly in the *Atparp* single and double mutants (Figure 7). To check if different repair pathways are used

in the different plant lines, the rejoining region was sequenced. Most of the ends had been joined precisely, but in some 1-3 bp had been deleted. No differences were observed between the *Atparp* mutants and the wild-type (data not shown). AtParp proteins have been shown to be involved in B-NHEJ in mammalian cells (11;14). When the C-NHEJ is functional, the deficiency in *AtParp* genes only has a minor influence on the end joining capacity of the cell.

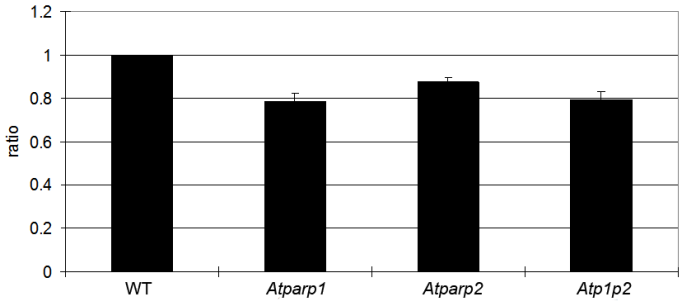

Figure 7. Plasmid end-joining assay.
Rejoined plasmid DNA with respect to total plasmid DNA in wild-type protoplasts was set on 1. Values of end joining in protoplasts from the mutants are given relative to that of the wild-type.

MMEJ assay

Since recent reports showed that Parp proteins are involved in B-NHEJ in mammalian cells (4;11;39;40) and that B-NHEJ is prone to utilize microhomology (41-43), we hypothesized that Parp proteins may be involved in MMEJ in plants as well. To test whether Parp proteins contribute to MMEJ, a MMEJ assay was performed. We expected to find less MMEJ products when Parp proteins are absent. Three hundred µg linear DNA substrates containing 10 bp repeats at the ends (Figure 2) were incubated without or with 1 µg protein extract from leaves of the *Atparp1*, *Atparp2*, *Atp1p2* mutants or the wild-type. The joined region was amplified by PCR with the primers flanking the junction (q30+q31), and with all extracts PCR products were obtained. No products were obtained in the absence of protein extract (data not shown). When end-joining occurs via MMEJ using the 10 bp microhomology, an XcmI site (CCAN9TGG) will be generated (Figure 2). To determine the fraction of the products joined via MMEJ using the 10 bp microhomology, the PCR products were digested with XcmI (Figure 8). We repeatedly saw a significant reduction in the amount of MMEJ products in the *Atp1p2* double mutant, corroborating with the requirement of AtParp proteins for MMEJ.

T-DNA integration

Double strand break repair mechanisms are hypothesized to control the integration of *Agrobacterium* T-DNA in plants. Though there is evidence to the contrary (35;44), some reports points to a role of C-NHEJ components in T-DNA integration in plants like this is the case in yeast (45;46). Our own previous data showed that in the *Atku80* and *Atku70* mutants the floral dip transformation frequency is significantly reduced compared with that

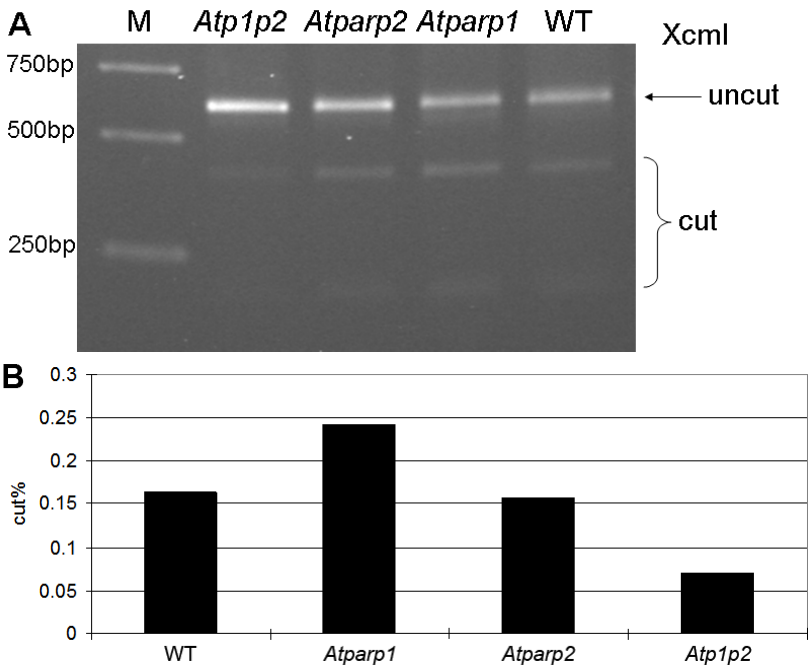

Figure 8. MMEJ catalyzed by protein extracts from leaves.
(A) A 600-bp fragment was PCR-amplified on the end-joined products and subsequently digested with XcmI. Only the products via MMEJ can be digested with XcmI resulting in two fragments of 400bp and 200bp.
(B) Quantification of MMEJ activity from (A). The relative contribution of MMEJ was calculated as the percentage of the XcmI-digested fragments of total PCR products (sum of the XcmI-digested and undigested fragments).

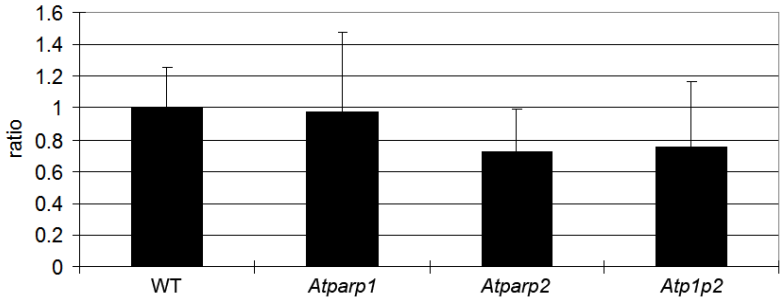

Figure 9. Transformation frequencies using the floral dip assay.
One gram of seeds from the wild-type and the NHEJ mutants obtained after floral dip transformations were selected on hygromycin. The number of hygromycin resistant seedlings was scored 2 weeks after germination. The transformation frequency is presented as the ratio of the percentage of hygromycin resistant seedlings in the mutants and the wild-type.

in the wild-type (chapter 2), but root transformation of the *Atku80*, *Atku70* and *Atlig4* mutants was as efficient as that of the wild-type (chapter2). To determine whether components which are involved in B-NHEJ, like AtParp1 and AtParp2, would also influence T-DNA

integration in plants, wild-type and *Atparp* mutants were transformed by *Agrobacterium* using the floral dip method. The transformation frequency was determined as the number of Hpt-resistant seedlings per total number of plated seeds. The transformation frequencies of the *Atparp* mutants were not significantly reduced compared with the wild-type (Figure 9), indicating that AtParp1 and AtParp2 are not essential for efficient T-DNA integration in germline cells. Since C-NHEJ is the major pathway of DSBs repair and consequently may have a major role in T-DNA integration as well, the influence of B-NHEJ is neglectable when C-NHEJ is functional.

Discussion

Here two T-DNA insertion mutants of AtParp1 and AtParp2 were isolated and characterized. There was no phenotypical difference under normal growth conditions between the *Atparp* mutants and the wild-type plants. Some former researchers showed that AtParp proteins were involved in programmed cell death (PCD) process and play a role in the stress tolerance (19-21). Our *Atparp* mutants were tested by drought, salt and cold stress, but no obvious differences were observed (data not shown) in contrast to the *Atparp*-deficient plants used by de Block *et al*. (19). These latter were however made by overexpression of *dsRNA-Atparp* constructs and this may have caused their different behavior.

Like their counterparts in animals, AtParp proteins were found to be involved in the process of DNA repair in Arabidopsis. The *Atparp1* mutant was hypersensitive to MMS, which mainly causes SSB, but was tolerant to bleomycin, which mainly causes DSB, indicating that AtParp1 plays an important role in SSB repair. Since all the components of C-NHEJ were present in the *Atparp* mutants, DSBs can be efficiently repaired via C-NHEJ and consequently the *Atparp* mutants could stand the stress from bleomycin. The *Atparp2* mutant could tolerate the genotoxic stress equally well as the wild-type, but the *Atp1p2* double mutant was more sensitive than the *Atparp1* mutant. It means that AtParp2 probably plays a minor role in DNA repair and its function only becomes apparent in the absence of AtParp1. In mice, single mutants of Parp1 or Parp2 can survive, but the double mutant is embryo lethal, suggesting that Parp1 and Parp2 are functionally redundant (47). Microarray data show that the expression level of *AtParp2* is increased in the *Atku80* mutant and in the wild-type after the treatment of bleomycin (23). The expression of *AtParp2* is thus possibly induced when there is DNA damage due to the absence of C-NHEJ. This was confirmed by the Q-RT-PCR results for RNA expression of *AtParp2* in NHEJ mutants. We also found similar enhanced expression of *AtParp1* and *AtXrcc1* in these NHEJ mutants. This would be in line with a response to the presence of DSBs and a role of AtParp and the scaffold protein AtXrcc1 in a backup pathway of DNA end joining.

Since C-NHEJ is still functional in the *Atparp* mutants, the end joining capacity was not significantly diminished in these mutants. Still the way the ends are joined is different from the wild-type. In the wild-type, two DNA ends containing micro-homology can be

joined using MMEJ. In the *Atp1p2* mutant, the products of MMEJ were obtained much less frequently than in the wild-type. In the *Atparp1* and *Atparp2* single mutants, more products of MMEJ were obtained than in the *Atp1p2* mutant. This indicated that the two AtParp proteins together play an important role in MMEJ and function redundantly. Recently Mansour *et al.* (14) reported that in mammals back-up NHEJ required Parp1, but was independent on microhomologies. Further work is needed to find out whether this is the case in plants as well. An analysis of the effect of the *Atparp* mutants in the background of C-NHEJ mutants may generate such insight. Blocking both the C-NHEJ and B-NHEJ pathways may also open possibilities to increase the efficiency of homologous recombination and thus of gene-targeting.

Reference List

1. Burzio,L.O., Riquelme,P.T. and Koide,S.S. (1979) ADP ribosylation of rat liver nucleosomal core histones. *J. Biol. Chem.*, **254**, 3029-3037.
2. Riquelme,P.T., Burzio,L.O. and Koide,S.S. (1979) ADP ribosylation of rat liver lysine-rich histone *in vitro*. *J. Biol. Chem.*, **254**, 3018-3028.
3. Ame,J.C., Spenlehauer,C. and de Murcia,G. (2004) The PARP superfamily. *Bioessays*, **26**, 882-893.
4. Yelamos,J., Schreiber,V. and Dantzer,F. (2008) Toward specific functions of poly(ADP-ribose) polymerase-2. *Trends Mol. Med.*, **14**, 169-178.
5. Woodhouse,B.C. and Dianov,G.L. (2008) Poly ADP-ribose polymerase-1: an international molecule of mystery. *DNA Repair (Amst)*, **7**, 1077-1086.
6. Cistulli,C., Lavrik,O.I., Prasad,R., Hou,E. and Wilson,S.H. (2004) AP endonuclease and poly(ADP-ribose) polymerase-1 interact with the same base excision repair intermediate. *DNA Repair (Amst)*, **3**, 581-591.
7. Satoh,M.S. and Lindahl,T. (1992) Role of poly(ADP-ribose) formation in DNA repair. *Nature*, **356**, 356-358.
8. Woodhouse,B.C., Dianova,I.I., Parsons,J.L. and Dianov,G.L. (2008) Poly(ADP-ribose) polymerase-1 modulates DNA repair capacity and prevents formation of DNA double strand breaks. *DNA Repair (Amst)*, **7**, 932-940.
9. Haince,J.F., McDonald,D., Rodrigue,A., Dery,U., Masson,J.Y., Hendzel,M.J. and Poirier,G.G. (2008) PARP1-dependent kinetics of recruitment of MRE11 and NBS1 proteins to multiple DNA damage sites. *J. Biol. Chem.*, **283**, 1197-1208.
10. Bryant,H.E., Petermann,E., Schultz,N., Jemth,A.S., Loseva,O., Issaeva,N., Johansson,F., Fernandez,S., McGlynn,P. and Helleday,T. (2009) PARP is activated at stalled forks to mediate Mre11-dependent replication restart and recombination. *EMBO J.*, **28**, 2601-2615.
11. Audebert,M., Salles,B. and Calsou,P. (2004) Involvement of poly(ADP-ribose) polymerase-1 and XRCC1/DNA ligase III in an alternative route for DNA double-strand breaks rejoining. *J. Biol. Chem.*, **279**, 55117-55126.
12. Audebert,M., Salles,B. and Calsou,P. (2008) Effect of double-strand break DNA sequence on the PARP-1 NHEJ pathway. *Biochem. Biophys. Res. Commun.*, **369**, 982-988.
13. Mortusewicz,O., Ame,J.C., Schreiber,V. and Leonhardt,H. (2007) Feedback-regulated poly(ADP-ribosyl)ation by PARP-1 is required for rapid response to DNA damage in living cells. *Nucleic Acids Res.*, **35**, 7665-7675.
14. Mansour,W.Y., Rhein,T. and Dahm-Daphi,J. (2010) The alternative end-joining pathway for repair of DNA double-strand breaks requires PARP1 but is not dependent upon microhomologies. *Nucleic Acids Res.*, **38**, 6065-6077.

15. Babiychuk,E., Cottrill,P.B., Storozhenko,S., Fuangthong,M., Chen,Y., O'Farrell,M.K., Van Montagu,M., Inze,D. and Kushnir,S. (1998) Higher plants possess two structurally different poly(ADP-ribose) polymerases. *Plant J.*, **15**, 635-645.
16. Chen,Y.M., Shall,S. and O'Farrell,M. (1994) Poly(ADP-ribose) polymerase in plant nuclei. *Eur. J. Biochem.*, **224**, 135-142.
17. Lepiniec,L., Babiychuk,E., Kushnir,S., van Montagu,M. and Inze,D. (1995) Characterization of an *Arabidopsis thaliana* cDNA homologue to animal poly(ADP-ribose) polymerase. *FEBS Lett.*, **364**, 103-108.
18. Ame,J.C., Rolli,V., Schreiber,V., Niedergang,C., Apiou,F., Decker,P., Muller,S., Hoger,T., Murcia,J.M. and de Murcia,G. (1999) PARP-2, A novel mammalian DNA damage-dependent poly(ADP-ribose) polymerase. *J. Biol. Chem.*, **274**, 17860-17868.
19. De Block,M., Verduyn,C., De Brouwer,D. and Cornelissen,M. (2005) Poly(ADP-ribose) polymerase in plants affects energy homeostasis, cell death and stress tolerance. *Plant J.*, **41**, 95-106.
20. Amor,Y., Babiychuk,E., Inze,D. and Levine,A. (1998) The involvement of poly(ADP-ribose) polymerase in the oxidative stress responses in plants. *FEBS Lett.*, **440**, 1-7.
21. Vanderauwera,S., De Block,M., Van de Steene,N., van de Cotte,B., Metzlaff,M. and Van Breusegem,F. (2007) Silencing of poly(ADP-ribose) polymerase in plants alters abiotic stress signal transduction. *Proc. Natl. Acad. Sci. U. S. A*, **104**, 15150-15155.
22. Doucet-Chabeaud,G., Godon,C., Brutesco,C., de Murcia,G. and Kazmaier,M. (2001) Ionising radiation induces the expression of PARP-1 and PARP-2 genes in Arabidopsis. *Mol. Genet. Genomics*, **265**, 954-963.
23. West,C.E., Waterworth,W.M., Sunderland,P.A. and Bray,C.M. (2004) Arabidopsis DNA double-strand break repair pathways. *Biochem. Soc. Trans.*, **32**, 964-966.
24. Alonso,J.M., Stepanova,A.N., Leisse,T.J., Kim,C.J., Chen,H., Shinn,P., Stevenson,D.K., Zimmerman,J., Barajas,P., Cheuk,R. *et al.* (2003) Genome-wide insertional mutagenesis of *Arabidopsis thaliana*. *Science*, **301**, 653-657.
25. de Pater,S., Caspers,M., Kottenhagen,M., Meima,H., ter Stege,R. and de Vetten,N. (2006) Manipulation of starch granule size distribution in potato tubers by modulation of plastid division. *Plant Biotechnol. J.*, **4**, 123-134.
26. Weijers,D., Franke-van Dijk,M., Vencken,R.J., Quint,A., Hooykaas,P. and Offringa,R. (2001) An Arabidopsis Minute-like phenotype caused by a semi-dominant mutation in a RIBOSOMAL PROTEIN S5 gene. *Development*, **128**, 4289-4299.
27. Menke,M., Chen,I., Angelis,K.J. and Schubert,I. (2001) DNA damage and repair in *Arabidopsis thaliana* as measured by the comet assay after treatment with different classes of genotoxins. *Mutat. Res.*, **493**, 87-93.
28. Takahashi,N., Lammens,T., Boudolf,V., Maes,S., Yoshizumi,T., de Jaeger,G., Witters,E., Inze,D. and de Veylder,L. (2008) The DNA replication checkpoint aids survival of plants deficient in the novel replisome factor ETG1. *EMBO J.*, **27**, 1840-1851.
29. Lindhout,B.I., Pinas,J.E., Hooykaas,P.J. and van der Zaal,B.J. (2006) Employing libraries of zinc finger artificial transcription factors to screen for homologous recombination mutants in Arabidopsis. *Plant J.*, **48**, 475-483.
30. Wang,S., Tiwari,S.B., Hagen,G. and Guilfoyle,T.J. (2005) AUXIN RESPONSE FACTOR7 restores the expression of auxin-responsive genes in mutant Arabidopsis leaf mesophyll protoplasts. *Plant Cell*, **17**, 1979-1993.
31. Liang,L., Deng,L., Nguyen,S.C., Zhao,X., Maulion,C.D., Shao,C. and Tischfield,J.A. (2008) Human DNA ligases I and III, but not ligase IV, are required for microhomology-mediated end joining of DNA double-strand breaks. *Nucleic Acids Res.*, **36**, 3297-3310.
32. Liang,L., Deng,L., Chen,Y., Li,G.C., Shao,C. and Tischfield,J.A. (2005) Modulation of DNA end joining by nuclear proteins. *J. Biol. Chem.*, **280**, 31442-31449.
33. Clough,S.J. and Bent,A.F. (1998) Floral dip: a simplified method for *Agrobacterium*-

mediated transformation of Arabidopsis thaliana. *Plant J.*, **16**, 735-743.
34. de Pater,S., Neuteboom,L.W., Pinas,J.E., Hooykaas,P.J. and van der Zaal,B.J. (2009) ZFN-induced mutagenesis and gene-targeting in Arabidopsis through *Agrobacterium*-mediated floral dip transformation. *Plant Biotechnol. J.*, **7**, 821-835.
35. van Attikum,H., Bundock,P., Overmeer,R.M., Lee,L.Y., Gelvin,S.B. and Hooykaas,P.J. (2003) The Arabidopsis AtLIG4 gene is required for the repair of DNA damage, but not for the integration of *Agrobacterium* T-DNA. *Nucleic Acids Res.*, **31**, 4247-4255.
36. Burger,R.M., Peisach,J. and Horwitz,S.B. (1981) Activated bleomycin. A transient complex of drug, iron, and oxygen that degrades DNA. *J. Biol. Chem.*, **256**, 11636-11644.
37. O'Connor,P.J. (1981) Interaction of chemical carcinogens with macromolecules. *J. Cancer Res. Clin. Oncol.*, **99**, 167-186.
38. Schreiber,V., Ame,J.C., Dolle,P., Schultz,I., Rinaldi,B., Fraulob,V., Murcia,J.M. and de Murcia,G. (2002) Poly(ADP-ribose) polymerase-2 (PARP-2) is required for efficient base excision DNA repair in association with PARP-1 and XRCC1. *J. Biol. Chem.*, **277**, 23028-23036.
39. Robert,I., Dantzer,F. and Reina-San-Martin,B. (2009) Parp1 facilitates alternative NHEJ, whereas Parp2 suppresses IgH/c-myc translocations during immunoglobulin class switch recombination. *J. Exp. Med.*, **206**, 1047-1056.
40. Wang,M., Wu,W., Wu,W., Rosidi,B., Zhang,L., Wang,H. and Iliakis,G. (2006) PARP-1 and Ku compete for repair of DNA double strand breaks by distinct NHEJ pathways. *Nucleic Acids Res.*, **34**, 6170-6182.
41. Verkaik,N.S., Esveldt-van Lange,R.E., van Heemst,D., Bruggenwirth,H.T., Hoeijmakers,J.H., Zdzienicka,M.Z. and van Gent,D.C. (2002) Different types of V(D) J recombination and end-joining defects in DNA double-strand break repair mutant mammalian cells. *Eur. J. Immunol.*, **32**, 701-709.
42. Simsek,D. and Jasin,M. (2010) Alternative end-joining is suppressed by the canonical NHEJ component Xrcc4-ligase IV during chromosomal translocation formation. *Nat. Struct. Mol. Biol.*, **17**, 410-416.
43. Fattah,F., Lee,E.H., Weisensel,N., Wang,Y., Lichter,N. and Hendrickson,E.A. (2010) Ku regulates the non-homologous end joining pathway choice of DNA double-strand break repair in human somatic cells. *PLoS. Genet.*, **6**, e1000855.
44. Gallego,M.E., Bleuyard,J.Y., Daoudal-Cotterell,S., Jallut,N. and White,C.I. (2003) Ku80 plays a role in non-homologous recombination but is not required for T-DNA integration in Arabidopsis. *Plant J.*, **35**, 557-565.
45. Li,J., Vaidya,M., White,C., Vainstein,A., Citovsky,V. and Tzfira,T. (2005) Involvement of KU80 in T-DNA integration in plant cells. *Proc. Natl. Acad. Sci. U. S. A*, **102**, 19231-19236.
46. Friesner,J. and Britt,A.B. (2003) Ku80- and DNA ligase IV-deficient plants are sensitive to ionizing radiation and defective in T-DNA integration. *Plant J.*, **34**, 427-440.
47. Menissier de Murcia,J., Ricoul,M., Tartier,L., Niedergang,C., Huber,A., Dantzer,F., Schreiber,V., Ame,J.C., Dierich,A., LeMeur,M. *et al.* (2003) Functional interaction between PARP-1 and PARP-2 in chromosome stability and embryonic development in mouse. *EMBO J.*, **22**, 2255-2263.